

Coplanar and noncoplanar nucleon-nucleon bremsstrahlung calculation: A study of pseudoscalar and pseudovector πN couplings

M. K. Liou and Yi Li

Department of Physics and Institute for Nuclear Theory, Brooklyn College of the City University of New York, Brooklyn, New York 11210

W. M. Schreiber

Department of Applied Sciences, The College of Staten Island of the City University of New York, Staten Island, New York 10314

R. W. Brown

Department of Physics, Case Western Reserve University, Cleveland, Ohio 44106

(Received 27 June 1995)

The $pp\gamma$ and $np\gamma$ processes have been used to study pseudoscalar (ps) and pseudovector (pv) πN couplings. We calculate both coplanar and noncoplanar cross sections using a realistic one-boson exchange model in the energy region between 100 and 300 MeV. We find that the difference in cross sections calculated using the two couplings increases as the nucleon scattering angles decrease. Furthermore, this difference becomes greater with increasing incident energy. We show for the $pp\gamma$ case that this difference will be significantly increased upon the inclusion of electromagnetic form factors. For $pp\gamma$ with large proton scattering angles ($\geq 30^\circ$), cross sections (both ps and pv) calculated using an on-shell $p\gamma p$ vertex are in very good agreement with the data, and they are also extremely close to a recent soft-photon calculation at 157 MeV using the two- u -two- t special amplitude. The ps and pv calculations are both in good agreement with the TRIUMF data at 200 and 280 MeV. More accurate data are required to differentiate between these two couplings. Agreement with sparsely available $np\gamma$ data is good for most cases, but discrepancies do exist for some data points. For large nucleon scattering angles, noncoplanar cross sections for both $np\gamma$ and $pp\gamma$ change rapidly with the noncoplanar angle. However, the respective shapes of the noncoplanar $np\gamma$ and $pp\gamma$ curves are very different.

PACS number(s): 25.40.-h, 13.40.-f, 13.75.Cs, 13.75.Gx

Nucleon-nucleon bremsstrahlung processes which include the $pp\gamma$ process

$$p(p_1^\mu) + p(p_2^\mu) \rightarrow p(p_3^\mu) + p(p_4^\mu) + \gamma(K^\mu),$$

and the $np\gamma$ process

$$p(p_1^\mu) + n(p_2^\mu) \rightarrow p(p_3^\mu) + n(p_4^\mu) + \gamma(K^\mu),$$

have been studied. We have calculated both coplanar and noncoplanar cross sections for these processes using a realistic OBE model obtained by Horowitz [1]. In these calculations the pion-nucleon coupling ($NN\pi$) has been treated not only as a pseudoscalar (ps) but also as a pseudovector (pv), i.e., $pp\gamma$ and $np\gamma$ cross sections have been calculated with the ps coupling ($\sigma_{pp\gamma}^{\text{ps}}$ and $\sigma_{np\gamma}^{\text{ps}}$) and the pv coupling ($\sigma_{pp\gamma}^{\text{pv}}$ and $\sigma_{np\gamma}^{\text{pv}}$). These processes have been studied both experimentally and theoretically during the past three decades [2]. Among various reasons for these studies, the most important one has been the investigation of the off-shell behavior of the two-nucleon interactions. The idea of using nucleon-nucleon bremsstrahlung as a tool for investigating the ps-pv problem is rather new, and it has never before been systematically studied. The main purposes and results of this paper are as follows. (i) To systematically study, for the first time, the change in bremsstrahlung cross section when the ps coupling is replaced by the pv coupling. We show that deviations in bremsstrahlung cross section, $\Delta_{pp\gamma} = \sigma_{pp\gamma}^{\text{ps}} - \sigma_{pp\gamma}^{\text{pv}}$ and $\Delta_{np\gamma} = \sigma_{np\gamma}^{\text{ps}} - \sigma_{np\gamma}^{\text{pv}}$, do not vanish because the respective nucleon has an anomalous magnetic moment

($\kappa_p = 1.79$ for proton and $\kappa_n = -1.91$ for neutron). It is well known that $\Delta_{pp\gamma}$ and $\Delta_{np\gamma}$ should be identically zero if those terms involving κ_p and κ_n are completely ignored [3,4]. We have found that the values of $\Delta_{pp\gamma}$ and $\Delta_{np\gamma}$ increase as the nucleon scattering angles decrease. This increase becomes more manifest with increasing incident energy. Moreover, the value of $\Delta_{pp\gamma}$ increases when the standard on-shell $p\gamma p$ vertex is replaced by an off-shell vertex. The results for both $\sigma_{pp\gamma}^{\text{ps}}$ and $\sigma_{pp\gamma}^{\text{pv}}$ are in good agreement with the TRIUMF data at 200 MeV [5] and 280 MeV [6]. The result at 280 MeV shows that more accurate data can be used to differentiate between the two couplings. (ii) To demonstrate that Horowitz's model, which fits the elastic data well, can be successfully used to describe the $pp\gamma$ and $np\gamma$ cross sections. (iii) To point out that the calculated $pp\gamma$ cross sections using an on-shell $p\gamma p$ vertex are in very close agreement with those calculated using a "two- u -two- t " special soft-photon amplitude M_μ^{TuTts} (but in gross disagreement with those calculated using a "two- s -two- t " special soft-photon amplitude M_μ^{TsTts}) [7]. (The definitions and nomenclature are explained in Refs. [7,8].) This is not surprising because it is easy to show that Horowitz's model can be used for the source diagrams to generate nucleon-nucleon bremsstrahlung processes at the tree level. The derived amplitude is obviously a two- u -two- t amplitude. If this amplitude is used as a guide to construct a more general soft-photon amplitude using a prescription discussed in a recent paper [8], then one would naturally obtain the M_μ^{TuTts} amplitude, not the M_μ^{TsTts} amplitude. Thus, the quantitative agreement between the two

calculations adds credence to the argument that M_{μ}^{TuTis} should be used to describe both $pp\gamma$ and $np\gamma$ processes [7]. (iv) To investigate the noncoplanarity effects in both $pp\gamma$ and $np\gamma$ processes. The information about the integrated cross section as a function of the noncoplanarity angle $\bar{\phi}$ is of significant experimental interest. We show that the noncoplanarity effects are quite different for $pp\gamma$ and $np\gamma$ processes. The noncoplanarity correction is found to be more important for those experiments which measure coplanar cross sections for large scattering angles ($\bar{\theta}_3 = \bar{\theta}_4 \geq 35^\circ$).

Our bremsstrahlung calculations are based on Horowitz's OBE model. In his paper, five Lorentz invariants were used to formulate the relativistic NN amplitudes. We do not directly use these five Lorentz invariants as input, and thus avoid the necessity of the inclusion of additional invariants to construct bremsstrahlung amplitudes. Instead, we have used Horowitz's parameters (masses, coupling constants, and cut-off parameters) for ten mesons to determine the OBE (tree) diagrams which are then used to generate $NN\gamma$ diagrams. We have chosen this approach mainly because (i) the internal emission amplitude can be easily obtained without ambiguity and (ii) the calculations of cross sections ($\sigma_{pp\gamma}^{ps}, \sigma_{np\gamma}^{ps}, \sigma_{pp\gamma}^{pv}, \sigma_{np\gamma}^{pv}$) are readily performed.

The derivation of the $pp\gamma$ amplitude ($M_{pp\gamma,\mu}^{ps}$ or $M_{pp\gamma,\mu}^{pv}$) from Horowitz's OBE model is straightforward. The amplitude takes into account photon emissions from four proton legs, but it does not have any contribution from neutral mesons exchanged between the two protons. Since the $np\gamma$ process involves not only the external emission from nucleon legs but also the internal emission from charged mesons exchanged between the proton and the neutron (the u -channel exchange), the $np\gamma$ amplitude ($M_{np\gamma,\mu}^{ps}$ or $M_{np\gamma,\mu}^{pv}$) does have a rather complicated internal amplitude. To find this internal amplitude we first attach a photon to the charged meson lines so that an expression for the internal contribution from those charged mesons can be obtained. Since the phenomenological form factors of the form

$$F(u_i) = \frac{\Lambda^2}{\Lambda^2 - u_i} \quad (i=1,2) \quad (1)$$

have been introduced in Horowitz's model, the internal amplitude is then the product of the expression obtained in the first step times the following gauge factor [9]:

$$F(u_1)F(u_2) \left[1 + \frac{m^2 - u_1}{\Lambda^2 - u_2} + \frac{m^2 - u_2}{\Lambda^2 - u_1} \right]. \quad (2)$$

In Eqs. (1) and (2), $u_1 = (p_1 - p_4)^2$, $u_2 = (p_2 - p_3)^2$, m is the mass of the exchanged meson and Λ is a cut-off parameter used in the model. For the case of pv coupling, the amplitude $M_{np\gamma,\mu}^{pv}$ must also include photon emissions from πN vertices.

Obviously, all four amplitudes $M_{\mu} (= M_{pp\gamma,\mu}^{ps}, M_{pp\gamma,\mu}^{pv}, M_{np\gamma,\mu}^{ps}, M_{np\gamma,\mu}^{pv})$ depend only upon relativistic invariants and they are fully gauge invariant. (We have also verified the gauge invariance of our numerical calculation, $M_{\mu} K^{\mu} \sim 10^{-20}$.) These amplitudes have been used to calculate the noncoplanar differential cross section $d^3\sigma/d\Omega_3 d\Omega_4 d\psi_{\gamma}$ as a function of the photon angle ψ_{γ} and the noncoplanarity angle $\bar{\phi}$ ($\bar{\phi}=0$ gives the coplanar cross

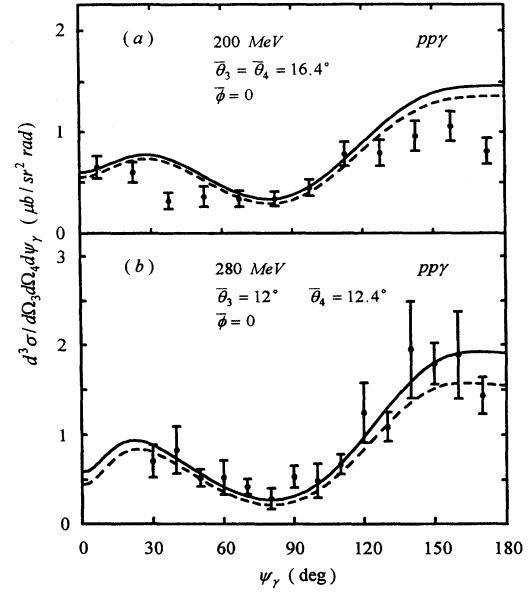


FIG. 1. Coplanar $pp\gamma$ cross section $d^3\sigma/d\Omega_3 d\Omega_4 d\psi_{\gamma}$ as a function of ψ_{γ} (a) at 200 MeV for $\bar{\theta}_3 = \bar{\theta}_4 = 16.4^\circ$ and (b) at 280 MeV for $\bar{\theta}_3 = 12^\circ$ and $\bar{\theta}_4 = 12.4^\circ$. The solid and dashed curves represent the results calculated using the ps and pv couplings, respectively. The data at 200 MeV are from [5], while the data at 280 MeV are from [6].

section). Specifically, for a given $\bar{\phi}$ (from zero to $\bar{\phi}_{\max}$), we calculate the differential cross sections $\sigma_{pp\gamma}^{ps}$, $\sigma_{pp\gamma}^{pv}$, $\sigma_{np\gamma}^{ps}$, and $\sigma_{np\gamma}^{pv}$ (all in the form $d^3\sigma/d\Omega_3 d\Omega_4 d\psi_{\gamma}$ as a function of ψ_{γ}) using the amplitudes $M_{pp\gamma,\mu}^{ps}$, $M_{pp\gamma,\mu}^{pv}$, $M_{np\gamma,\mu}^{ps}$, and $M_{np\gamma,\mu}^{pv}$, respectively. Note that the Harvard geometry [10,11] has been used to define all angles used in this work; we follow the definitions and most of the notations given in the Appendix of Ref. [10]. We have also integrated these differential cross sections over ψ_{γ} to obtain the integrated cross sections ($d^2\sigma/d\Omega_3 d\Omega_4$) as a function of $\bar{\phi}$.

It is clear that the OBE model provides the most direct and simple method to study the difference between $\sigma_{pp\gamma}^{ps}$ ($\sigma_{np\gamma}^{ps}$) and $\sigma_{pp\gamma}^{pv}$ ($\sigma_{np\gamma}^{pv}$). As we have already mentioned, our calculations are based on Horowitz's model [1]. In Ref. [1] two sets of parameters (at 135 MeV and 200 MeV) are given below the pion production threshold. Parameters for 300 MeV are also available (Horowitz, unpublished). Accordingly, our study has focused on the energy region between 100 and 300 MeV.

Some important results are shown in Figs. 1–5. In each figure, the cross sections calculated using the ps coupling are compared with those calculated using the pv coupling. These two calculations are also compared with the experimental data and/or the results calculated using other approaches.

In Fig. 1(a), we present the coplanar $pp\gamma$ cross section $d^3\sigma/d\Omega_3 d\Omega_4 d\psi_{\gamma}$ at 200 MeV as a function of ψ_{γ} for $\bar{\theta}_3 = \bar{\theta}_4 = 16.4^\circ$. The cross section $\sigma_{pp\gamma}^{ps}$ calculated with the ps coupling and the cross section $\sigma_{pp\gamma}^{pv}$ calculated with the pv coupling have a similar shape, but $\sigma_{pp\gamma}^{ps}$ is always greater than $\sigma_{pp\gamma}^{pv}$. Agreement with the TRIUMF data [5] is good for both cases, except for $\psi_{\gamma} \geq 140^\circ$. Though $\sigma_{pp\gamma}^{pv}$ appears to be in somewhat better agreement with the data than $\sigma_{pp\gamma}^{ps}$, the

experimental uncertainties are greater than the deviation $\Delta_{pp\gamma}$. Thus the TRIUMF result presented is not sufficiently sensitive to differentiate between the two calculations. However, $\Delta_{pp\gamma}$ increases dramatically if off-shell effects in the $p\gamma p$ vertex are taken into account. More precisely, all calculations presented in this work are based on the well-known on-shell vertex, $\Gamma_\mu = \gamma_\mu - i\kappa_p \sigma_{\mu\nu} K^\nu / (2m_p)$, where m_p is the proton mass. The off-shell $p\gamma p$ vertex has the form

$$\begin{aligned} & \bar{u}(p)\Gamma_\mu^{\text{off}}(p, p+K) \\ &= \bar{u}(p) \left\{ \gamma_\mu - \frac{i\sigma_{\mu\nu}K^\nu}{2m_p} \left[F_2^+(w^2) \frac{\not{p} + \not{K} + m_p}{2m_p} \right. \right. \\ & \quad \left. \left. + F_2^-(w^2) \frac{-\not{p} - \not{K} + m_p}{2m_p} \right] \right\}, \end{aligned} \quad (3)$$

where F_2^+ and F_2^- are two electromagnetic form factors which are functions of $w^2 = (p+K)^2$. In the limit $w^2 \rightarrow m_p^2$ we have $F_2^+(w^2) \rightarrow \kappa_p$ and $F_2^-(w^2) \rightarrow \lambda^-$ (an unknown constant). Nyman [12] has studied the dependence of the $pp\gamma$ cross section on the form factors using a formula obtained from a once-subtracted dispersion relation for F_2^- , i.e., $F_2^-(w^2) = \lambda^- + 2m_p[F_2^+(w^2) - \kappa_p]/m_\pi$, where m_π is the pion mass. Using Nyman's equation and denoting these calculations as barred we obtain the following results: (i) $\bar{\Delta}_{pp\gamma}$ is always greater than $\Delta_{pp\gamma}$ for any value of λ^- in the whole range of ψ_γ , especially in the region $\psi_\gamma \geq 140^\circ$. (ii) $\bar{\sigma}_{pp\gamma}^{\text{pv}}$ which varies rather slowly with the variation of λ^- (-1 to 4) in the whole range of ψ_γ is in good agreement with the TRIUMF data but it is not significantly different from $\sigma_{pp\gamma}^{\text{pv}}$. (iii) $\bar{\sigma}_{pp\gamma}^{\text{ps}}$ varies slowly with λ^- (-1 to 0) and is slightly higher than $\sigma_{pp\gamma}^{\text{ps}}$ in the region of $0 \leq \psi_\gamma \leq 120^\circ$. $\bar{\sigma}_{pp\gamma}^{\text{ps}}$ increases significantly (especially in the region $\psi_\gamma > 120^\circ$) as the absolute value of λ^- increases ($|\lambda^-| > 1$) and the agreement with the data gets worse. What we wish to emphasize here is that the deviation $\Delta_{pp\gamma}$ increases if we take into account the electromagnetic form factors. For this reason we believe that the $pp\gamma$ process with small proton scattering angles can be used to differentiate between the two couplings.

The value of $\Delta_{pp\gamma}$ increases as the incident proton energies increase. To demonstrate this fact we have calculated the $pp\gamma$ cross sections at 280 MeV for $\bar{\theta}_3 = 12^\circ$ and $\bar{\theta}_4 = 12.4^\circ$ using the on-shell $p\gamma p$ vertex and Horowitz's parameters at 300 MeV (unpublished). The calculated cross sections ($\sigma_{pp\gamma}^{\text{ps}}$ and $\sigma_{pp\gamma}^{\text{pv}}$), compared with the recent TRIUMF data (including 2/3 normalization factor) [6], are exhibited in Fig. 1(b). Again, the most sensitive region to differentiate between the two couplings is $130^\circ \leq \psi_\gamma \leq 180^\circ$. In this region, the values of $\Delta_{pp\gamma}$ are comparable to the uncertainties in the TRIUMF data. This encouraging result together with the overall very good agreement between the theory and experiment supports our claim that more accurate data around these energies and scattering angles could be used to distinguish the ps and pv couplings.

The noncoplanar $pp\gamma$ cross sections at 200 MeV as a function of ψ_γ for $\bar{\theta}_3 = \bar{\theta}_4 = 16.4^\circ$ and several noncoplanarity angles $\bar{\phi}$ have also been calculated. From these calculations we have found that the deviation $\Delta_{pp\gamma}$ does not change too much as the noncoplanarity angle $\bar{\phi}$ increases. This fact can

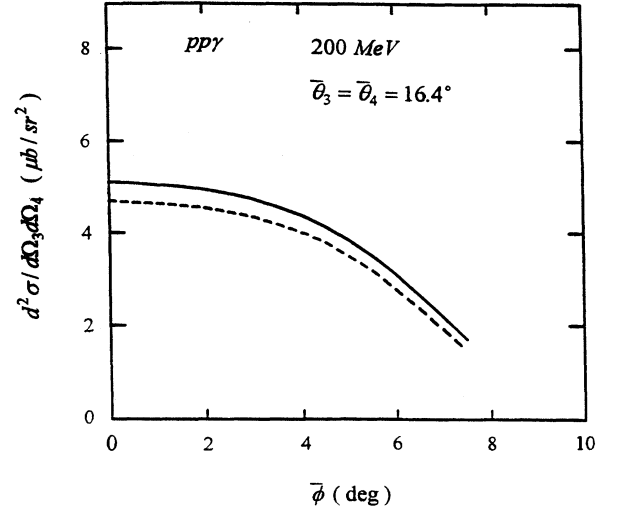


FIG. 2. Integrated $pp\gamma$ cross section $d^2\sigma/d\Omega_3d\Omega_4$ as a function of noncoplanarity angle $\bar{\phi}$ at 200 MeV for $\bar{\theta}_3 = \bar{\theta}_4 = 16.4^\circ$. The solid and dashed curves are the results for the ps and pv couplings, respectively.

be seen from Fig. 2, which shows the integrated cross section $d^2\sigma/d\Omega_3d\Omega_4$ as a function of $\bar{\phi}$.

In order to make a more detailed comparison with experiment we show the photon angular distribution $d^3\sigma/d\Omega_3d\Omega_4d\psi_\gamma$ at 157 MeV for $\bar{\theta}_3 = \bar{\theta}_4 = 30^\circ$ and several noncoplanarity angles $\bar{\phi}$ in Fig. 3. In this figure, $\sigma_{pp\gamma}^{\text{ps}}$ and $\sigma_{pp\gamma}^{\text{pv}}$ are compared with the Harvard data [11] and also with the result calculated using the Hamada-Johnston potential. The deviation $\Delta_{pp\gamma}$ is small, and both calculations agree very well with the data. Our results are also in close agreement with the HJ potential calculations [10,13].

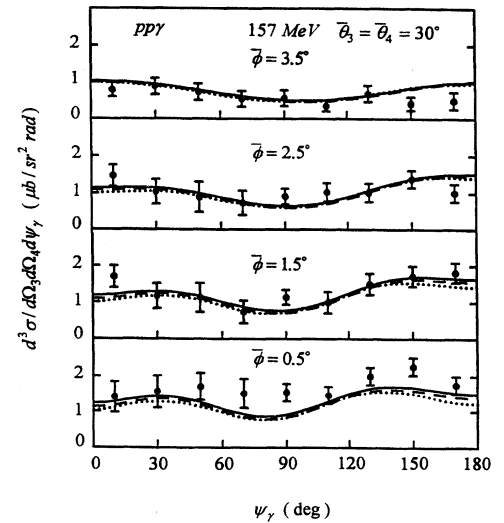


FIG. 3. Noncoplanar $pp\gamma$ cross section $d^3\sigma/d\Omega_3d\Omega_4d\psi_\gamma$ as a function of ψ_γ at 157 MeV for $\bar{\theta}_3 = \bar{\theta}_4 = 30^\circ$ and several noncoplanarity angles $\bar{\phi}$. The results for the ps coupling (solid curve) and pv coupling (dashed curve) are compared with the result calculated using the HJ potential (dotted curve) [10]. The data are from [11].

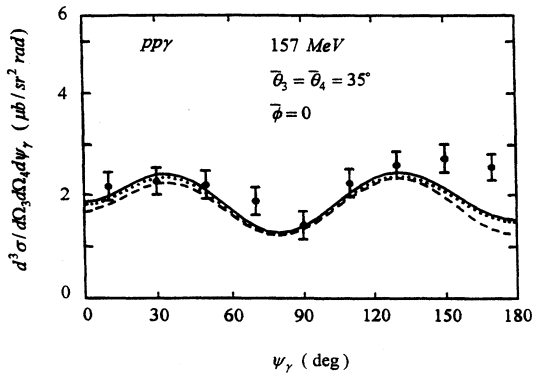


FIG. 4. Coplanar $pp\gamma$ cross section $d^3\sigma/d\Omega_3d\Omega_4d\psi_\gamma$ as a function of ψ_γ at 157 MeV for $\bar{\theta}_3=\bar{\theta}_4=35^\circ$. The results for the ps coupling (solid curve) and pv coupling (dashed curve) are compared with the soft-photon calculation using an amplitude M_μ^{TuTts} [7]. The data are from [11].

The comparison with other predictions is shown in Fig. 4. Note the quantitative agreement between our OBE result and the recent soft-photon calculations using the two- u -two- t special amplitude M_μ^{TuTts} [7]. Although not shown in the figure, our OBE result disagrees completely with the calculation using the two- s -two- t special amplitude M_μ^{TsTts} [7]. Thus M_μ^{TuTts} , not M_μ^{TsTts} , should be used to describe the nucleon-nucleon bremsstrahlung processes.

Our result for the $np\gamma$ case at 200 MeV is summarized in Fig. 5. In this figure we present the integrated cross section $d^2\sigma/d\Omega_3d\Omega_4$ as a function of the noncoplanarity angle $\bar{\phi}$ for $\bar{\theta}_3=\bar{\theta}_4=30^\circ, 35^\circ$, and 38° . Some interesting features can be observed. (i) The deviation $\Delta_{np\gamma}$ is extremely small for all cases, suggesting that the $np\gamma$ process with large scattering angles cannot be used to resolve the ps-pv problem. (ii) The shape of the noncoplanar curves shown in this figure for the $np\gamma$ case is quite different from that of the curve for the $pp\gamma$ case shown in Fig. 2. A similar feature has been obtained by other authors [14,15]. These curves indicate that the experimentally detected bremsstrahlung events must be corrected in order to determine the true coplanar cross sections, and the correction factor for the $np\gamma$ case is quite different from that for the $pp\gamma$ case. This noncoplanarity effect may explain the large discrepancy between all theoretical predictions and the experimental data [16] for $\bar{\theta}_3=\bar{\theta}_4=38^\circ$. (iii) Our coplanar results (both differential and integrated cross sections) are in close agreement with the calculations reported in Ref. [13] for $\bar{\theta}_3=\bar{\theta}_4=30^\circ, 35^\circ$, and 38° . We have also found that our

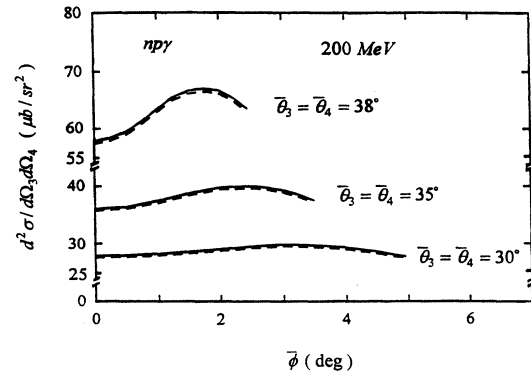


FIG. 5. Integrated $np\gamma$ cross section $d^2\sigma/d\Omega_3d\Omega_4$ as a function of $\bar{\phi}$ at 200 MeV for $\bar{\theta}_3=\bar{\theta}_4=30^\circ, 35^\circ$, and 38° . The solid and dashed curves represent the results for the ps and pv couplings, respectively.

photon angular distributions have very similar shapes to that obtained by Brown and Franklin [17], except that one of our double peaks is about 20–30 % smaller than their peak. (iv) Our coplanar predictions are consistently lower than those calculated by Schäfer *et al.* [3] even though both groups have used Horowitz's parameters as input. (The difference between the two calculations is almost a constant.) (v) We compared our result with many other predictions calculated using various models and approximations. Surprisingly, large discrepancies exist among these calculations, especially for those cases having large asymmetric angles.

In conclusion, we suggest that more precise $pp\gamma$ and $np\gamma$ experiments with small nucleon scattering angles should be performed. The measured cross sections can be used to investigate off-shell effects. The $pp\gamma$ data can be used to study the ps-pv problem and electromagnetic form factors. The $np\gamma$ data can be used to test various predictions calculated from different models and approximations, and will have implications relevant to the ps-pv problem.

We wish to thank Professor N. Chencinski and V. Grossman of the College of Staten Island for their assistance on numerical aspects of this work. We would also like to thank Professor C. J. Horowitz for communicating with us his unpublished parameters at 300 MeV. The work of M.K.L. was supported in part by the City University of New York Professional Staff Congress-Board of Higher Education Faculty Research Award Program, while the work of R.W.B. was supported in part by NSF and the CWRU industrial problem solving group. Summer matching funds provided by the College of Staten Island are greatly appreciated.

- [1] C. J. Horowitz, Phys. Rev. C **31**, 1340 (1985).
- [2] An extensive list of references can be obtained in Ref. [7].
- [3] M. Schäfer, T. S. Biro, W. Cassing, U. Mosel, H. Nifenecker, and J. A. Pinston, Z. Phys. A **339**, 391 (1991).
- [4] F. Villars, Helv. Phys. Acta **20**, 476 (1947).
- [5] J. G. Rogers *et al.*, Phys. Rev. C **22**, 2512 (1980).
- [6] K. Michaelian *et al.*, Phys. Rev. D **41**, 2689 (1990).

- [7] M. K. Liou, R. Timmermans, and B. F. Gibson, Phys. Lett. B **345**, 372 (1995). Note that the figures and captions do not match. The figures shown with the captions Fig. 1, Fig. 2, and Fig. 3 are actually Figs. 3, 1, and 2, respectively.
- [8] M. K. Liou, D. Lin, and B. F. Gibson, Phys. Rev. C **47**, 973 (1993).
- [9] I. S. Towner, Phys. Rep. **155**, 263 (1987).

- [10] M. K. Liou and M. I. Sobel, *Ann. Phys. (N.Y.)* **72**, 323 (1972).
- [11] B. Gottschalk, W. J. Schlaer, and K. H. Wang, *Nucl. Phys.* **A94**, 491 (1967).
- [12] E. M. Nyman, *Nucl. Phys.* **A160**, 517 (1971); **A154**, 97 (1970).
- [13] V. Herrmann, J. Speth, and K. Nakayama, *Phys. Rev. C* **43**, 394 (1991).
- [14] R. Baier, H. Kühnelt, and P. Urban, *Nucl. Phys.* **B11**, 675 (1969).
- [15] L. S. Celenza, B. F. Gibson, M. K. Liou, and M. I. Sobel, *Phys. Lett.* **41B**, 283 (1972).
- [16] F. P. Brady and J. C. Young, *Phys. Rev. C* **2**, 1579 (1970).
- [17] V. R. Brown and J. Franklin, *Phys. Rev. C* **8**, 1706 (1973).